CSMFO LAB. CHARACTERIZATION and DEVELOPMENT of MATERIALS for PHOTONICS and OPTOELECTRONICS Laboratory

Consiglio Nazionale delle Ricerche

DSFTM
Dipartimento di Scienze Fisiche e Tecnologie della Materia

IFN
Unità di Trento
www.tn.ifn.cnr.it

FONDAZIONE BRUNO KESSLER

Er^{3+} doped monolithic 1-D dielectric microcavity fabricated by rf-sputtering for coherent emission at 1.5 μm

A. Chiasera[1,*], F. Scotognella[2,3], Y.G. Boucher[4], G. Galzerano[5], A. Lukowiak[6], D.Ristic[7], G. Speranza[8,1], I. Vasilchenko[9], A. Vaccari[10], S. Valligatla[11], C. Meroni[12,1], S. Varas[1], L. Zur[13,1], M. Ivanda[7], G. C. Righini[13,14], S. Taccheo[15], R. Ramponi[5], M. Ferrari[1,13]

[1] IFN - CNR CSMFO Lab. & FBK CMM, via alla Cascata 56/C Povo, 38123 Trento, Italy.
[2] Politecnico di Milano, Dip. Fisica and IFN-CNR, Piazza Leonardo da Vinci 32, 20133, Milano, Italy
[3] Center for Nano Science and Technology@PoliMi, IIT, Via Giovanni Pascoli, 70/3, 20133, Milan, Italy
[4] Laboratoire FOTON (UMR CNRS 6082) Équipe Systèmes Photoniques, ENSSAT, CS 80518, F-22305 LANNION, France.
[5] IFN – CNR and Politecnico di Milano, Dip. Fisica, Piazza Leonardo da Vinci 32, 20133, Milano, Italy
[6] Institute of Low Temperature and Structure Research, PAS, 2 Okolna St., 50-422, Wroclaw, Poland
[7] Center of Excellence for Advanced Materials and Sensing Devices, Ruđer Bošković Institute, Bijenička c. 54, Zagreb, Croatia
[8] FBK CMM FMPS Unit, via Sommarive 18, Povo, 38123 Trento, Italy.
[9] Institute of High Technology Physics, Tomsk Polytechnic University, Tomsk, Russia.
[10] FBK CMM-ARES Unit, via Sommarive 18, Povo, 38123 Trento, Italy.
[12] Dipartimento di Fisica, Università di Trento, via Sommarive 14, Povo, 38123, Trento, Italy
[11] Institute for Integrative Nanosciences, IFW Dresden, Helmholtz Straße 20, 01069 Dresden, Germany.
[13] Enrico Fermi Center, Piazza del Viminale 1, 00184 Roma, Italy
[14] MiPLab. IFAC - CNR, Via Madonna del Piano 10, 50019 Sesto Fiorentino, Italy
[15] College of Engineering, Swansea University, Singleton Park, Swansea, UK

CHARACTERIZATION and DEVELOPMENT of MATERIALS for PHOTONICS and OPTOELECTRONICS Laboratory

www.tn.ifn.cnr.it

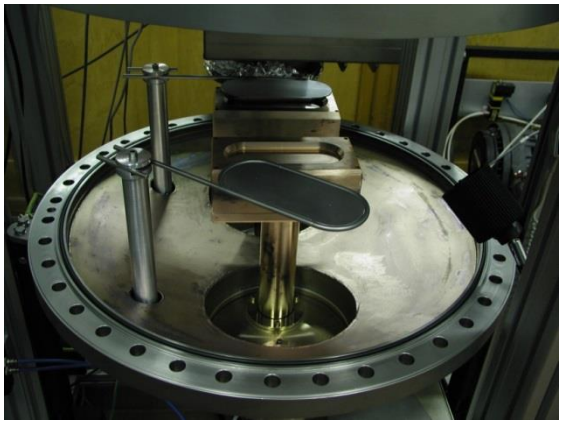

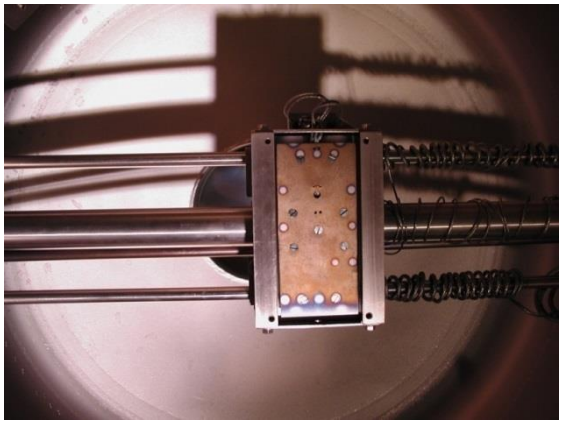

RF-Sputtering deposition

Deposition apparatus

- 2 rectangular Magnetron
- 2 Power supplier + 2 automatic matching box
- Cooling close circuit dedicated to the magnetrons
- The Ar gas flow during the deposition is controlled by automatic valve
- Sample holder (10 x 6 cm) with thermometer and heater (max 100°C)
- 20 cm distance between target and substrate
- Oil-free pumping system
- Reaction chamber + Pre chamber with cleaning of the substrate (heating up to 120°C)
- PC monitor and control the main operations during the deposition process

Viable Materials

- ✓ SiO_2; TiO_2; HfO_2; GeO_2; ZrO_2; TeO_2; ZnO_2; W_2O_3
- ✓ SiO_2-TiO_2; SiO_2-HfO_2; SiO_2-GeO_2
- ✓ Er; Yb; Dy; Eu; Ho; Nd; Sm; Tb; Tm;

Thickness monitor

- ❖ 2 quartz microbalance faced on the 2 targets
- ❖ Calibration on SiO_2 and TiO_2 films of thickness of more that 1 μm by mline apparatus
- ❖ Resolution ~1Å

1-D microcavities fabricated by RF-sputtering

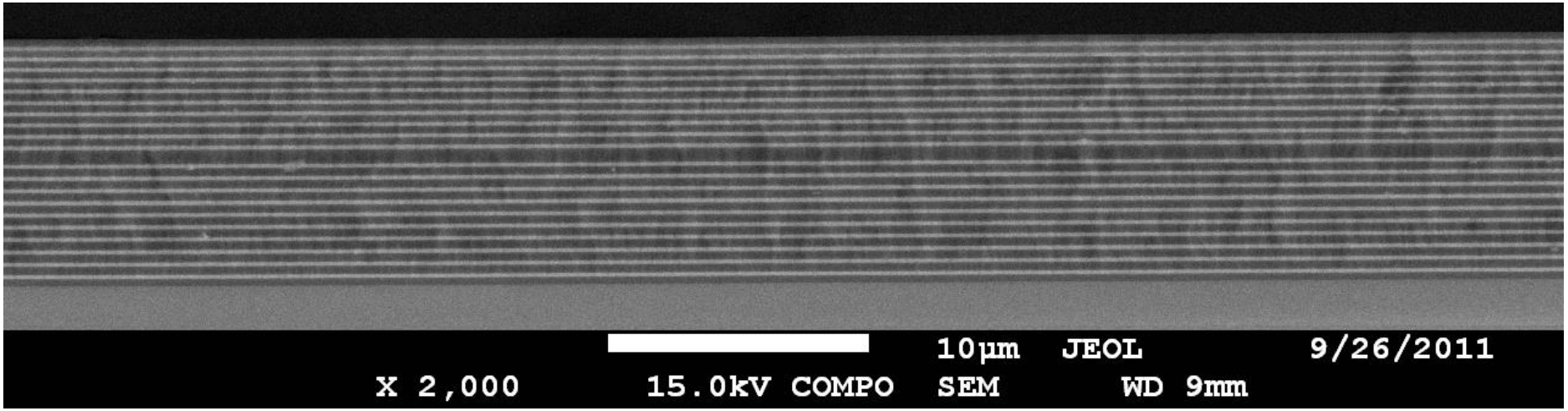

Bragg Mirror: 20 alternated quarter wave layers TiO_2 (170 nm) and SiO_2 (320 nm).

Active layer: half wave (640 nm) SiO_2 activated with 0.2 mol % of Er^{3+}.

The dark regions corresponds to SiO_2 and the white regions corresponds to TiO_2

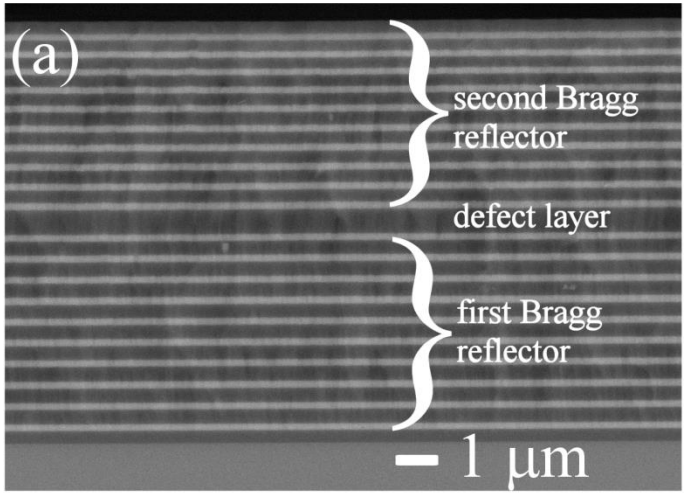

- S. Valligatla, A. Chiasera, S. Varas, N. Bazzanella, D.N. Rao, G.C. Righini, M. Ferrari, "High quality factor 1-D Er^{3+}-activated dielectric microcavity fabricated by RF-sputtering", Optics Express 20(19), 21214-21222 (2012)
- A. Chiasera, F. Scotognella, L. Criante, S. Varas, G. Della Valle, R. Ramponi, M. Ferrari, "Disorder in Photonic Structures Induced by Random Layer Thickness", Sci. Adv. Mater. 7 (2015) 1207-1212.
- S. Valligatla, A. Chiasera, S. Varas, P. Das, B.N.S. Bhaktha, A. Lukowiak, F. Scotognella, D.N. Rao, R. Ramponi, G.C. Righini, M. Ferrari, "Optical field enhanced nonlinear absorption and optical limiting properties of 1-D dielectric photonic crystal with ZnO defect", Optical Materials 50 (2015) pp. 229-233.

Transmission measurements

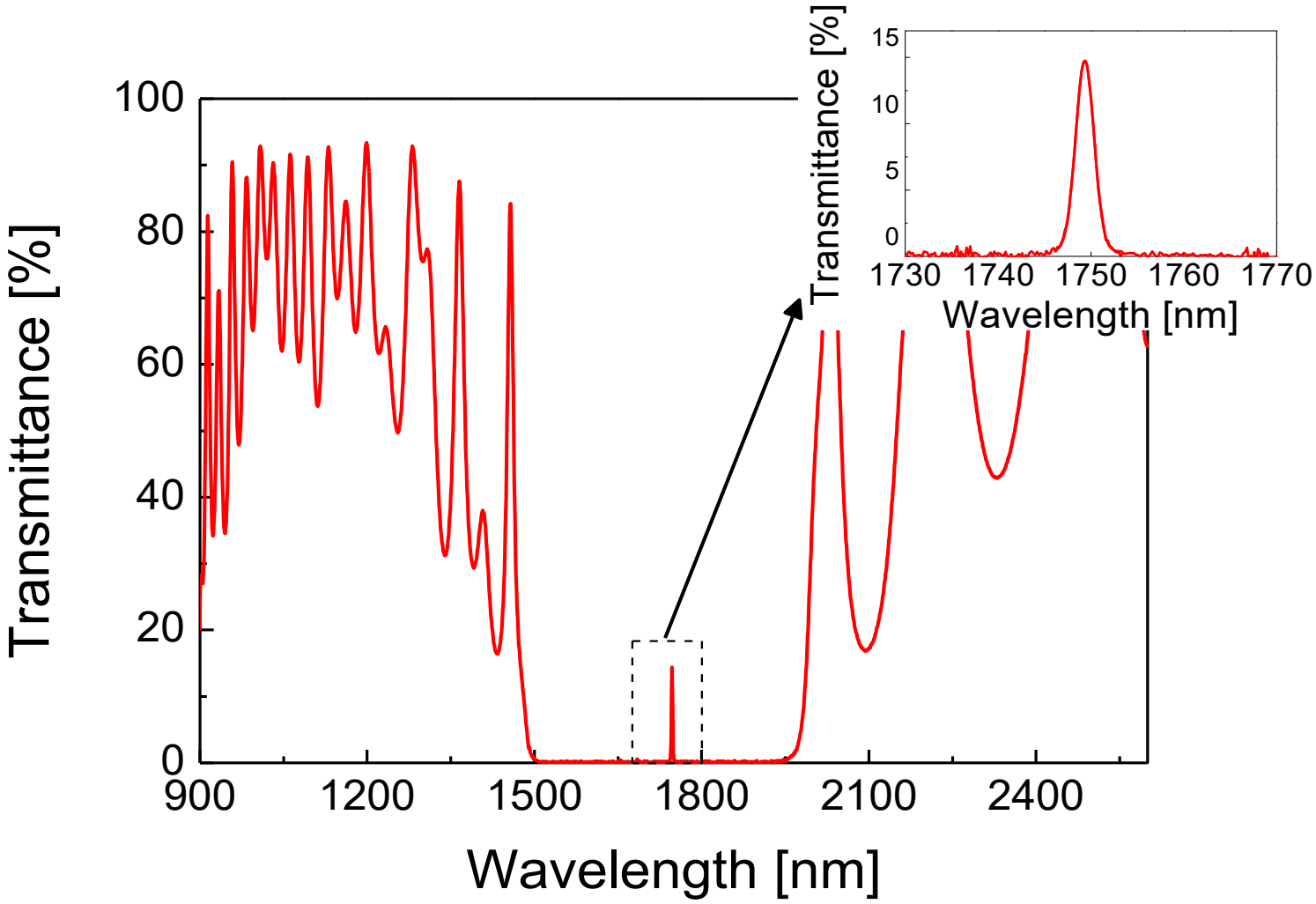

Transmittance spectrum of the cavity with two Bragg reflectors. The stop band range from 1490 to 1980 nm. The cavity resonance corresponds to the sharp maximum centred at 1.749 mm. The line width of the resonance is 1.97 nm that correspond to a quality Q factor of 890.

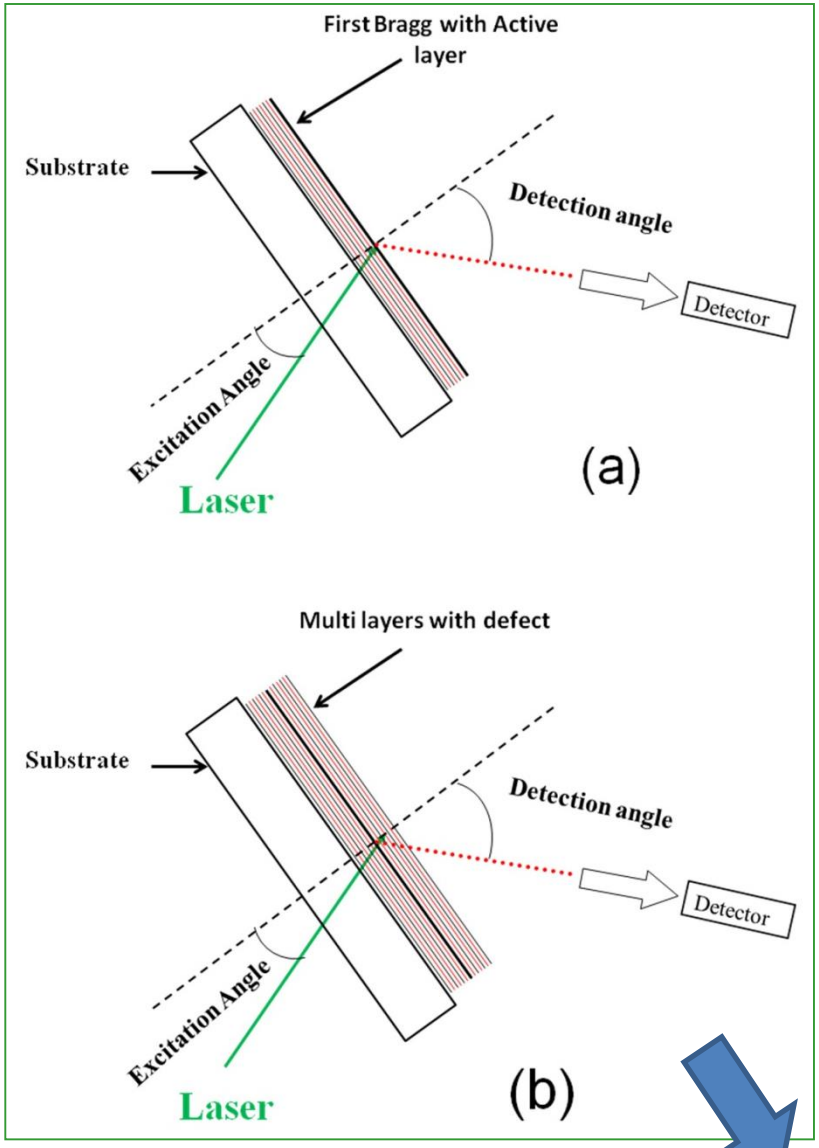

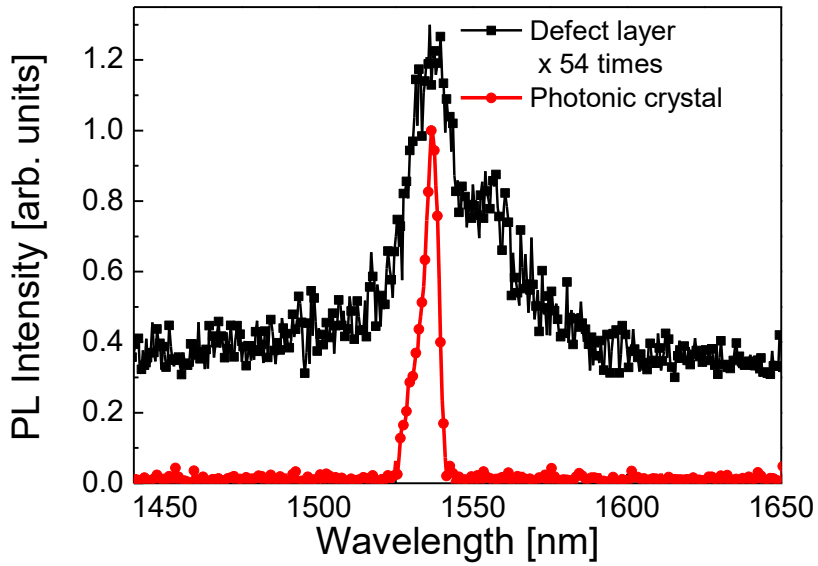

$^4I_{13/2} \rightarrow {}^4I_{15/2}$ photoluminescence spectra of the cavity activated by Er^{3+} ion in 1-D photonic crystal and of the single Er^{3+}-doped SiO_2 active layer with first Bragg mirror. The light is recorded at 50° from the normal on the samples upon excitation at 514.5 nm.

Schematics of the excitation and detection geometries employed for a reliable assessment of the influence of the cavity on the 1.5 mm emission band of Er^{3+} ion.

Fig. (a): configuration for the Er^{3+}-activated reference sample:
Fig. (b): configuration for the Er^{3+}-activated 1-D microcavity.

Coherent emission from fully Er^{3+} doped monolithic 1-D dielectric microcavity fabricated by rf-sputtering

Coherent emission from fully Er^{3+} doped monolithic 1-D dielectric microcavity fabricated by rf-sputtering

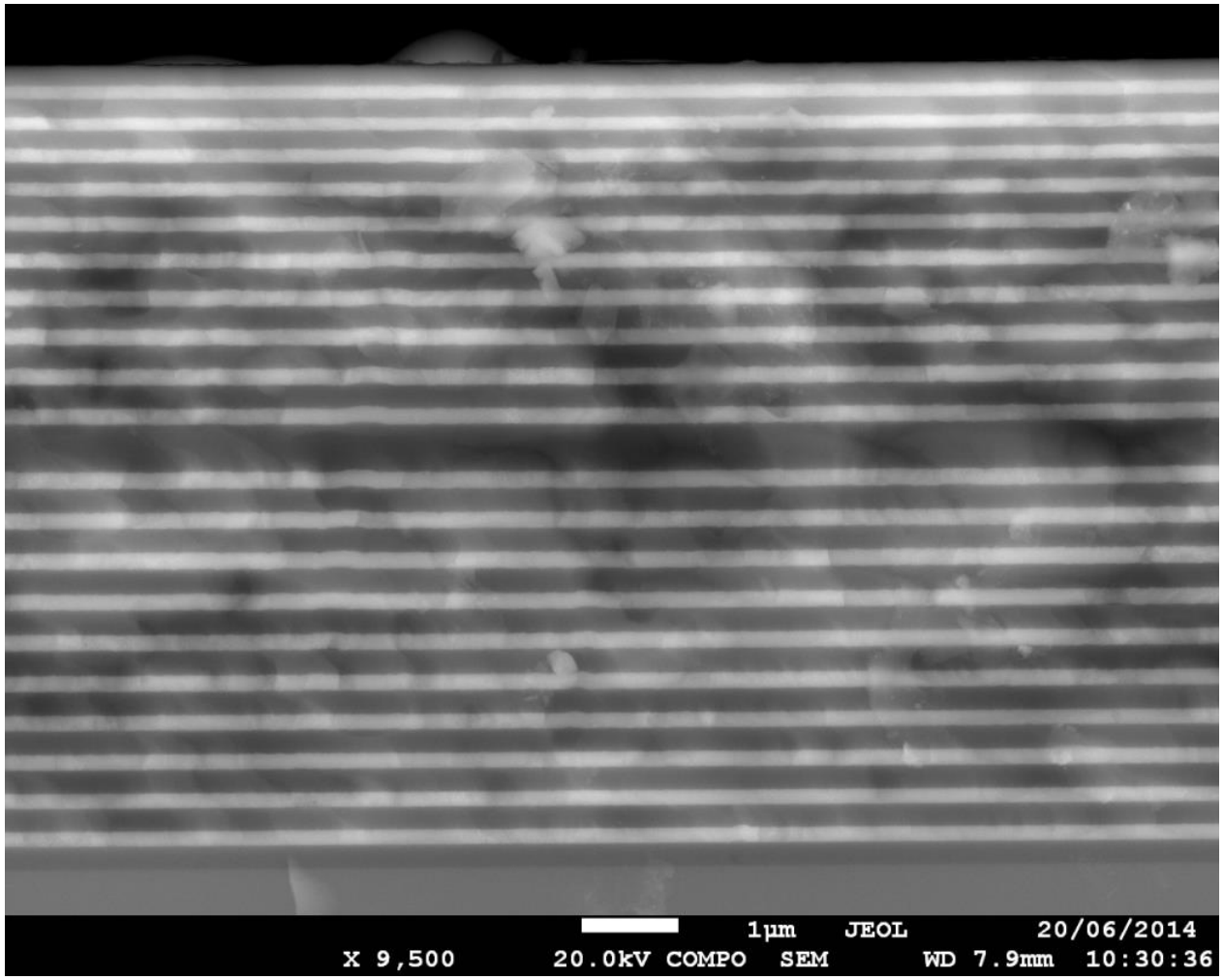

SEM micrograph of the Er^{3+} doped 1D dielectric microcavity cross section. The bright and dark region corresponds to TiO_2 and SiO_2 layers, respectively. The substrate is located on the bottom of the images and air on the top.

Transmission

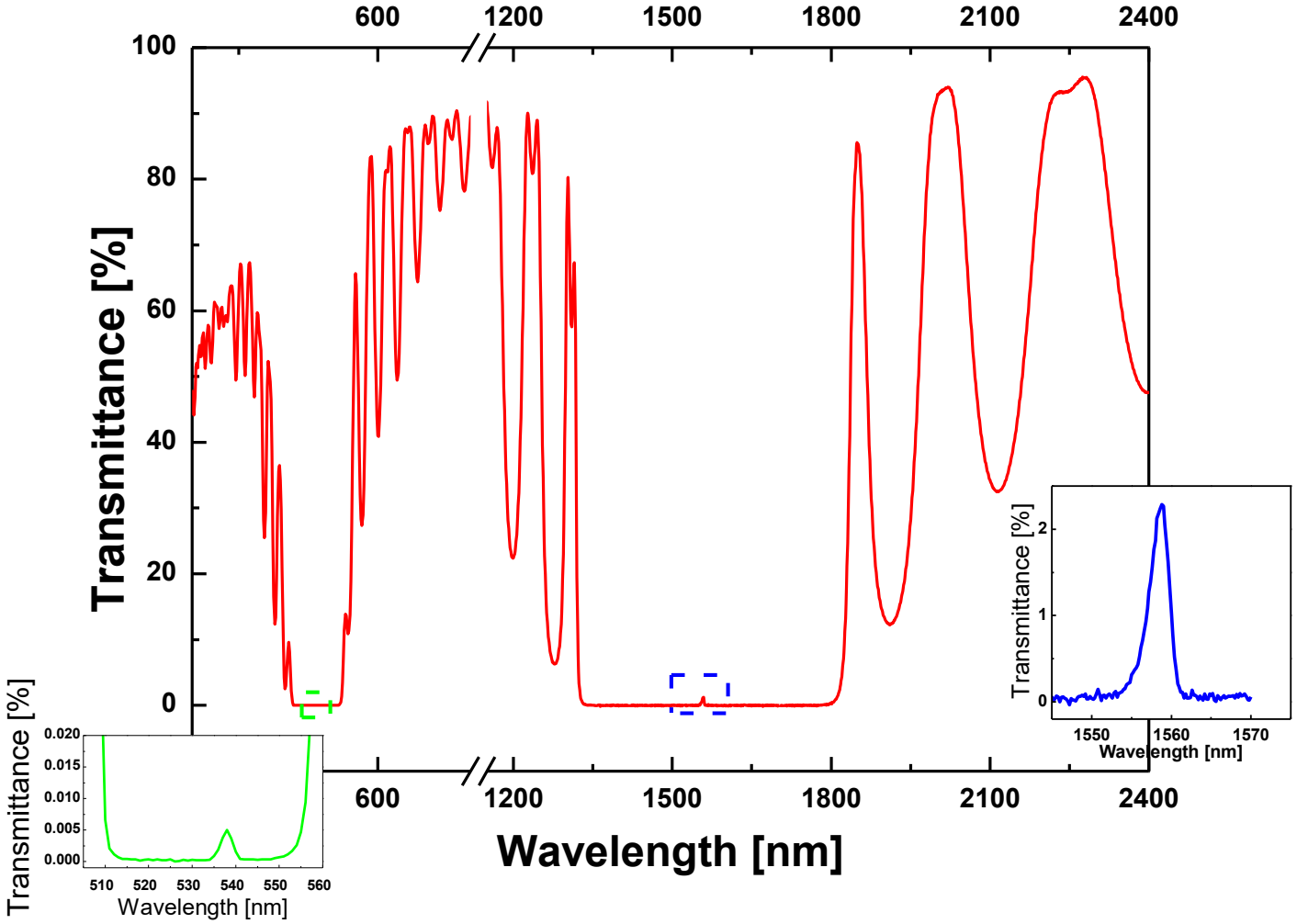

The first order stop band ranges from 1300 nm to 1850 nm. The first order cavity resonance corresponds to the sharp maximum centered at 1559.2 nm. Transmission spectra representing third order stop band in the visible region between 500 nm to 560 nm with third order cavity resonance at 536 nm.

$^4I_{13/2} \rightarrow {}^4I_{15/2}$ photoluminescence spectrum

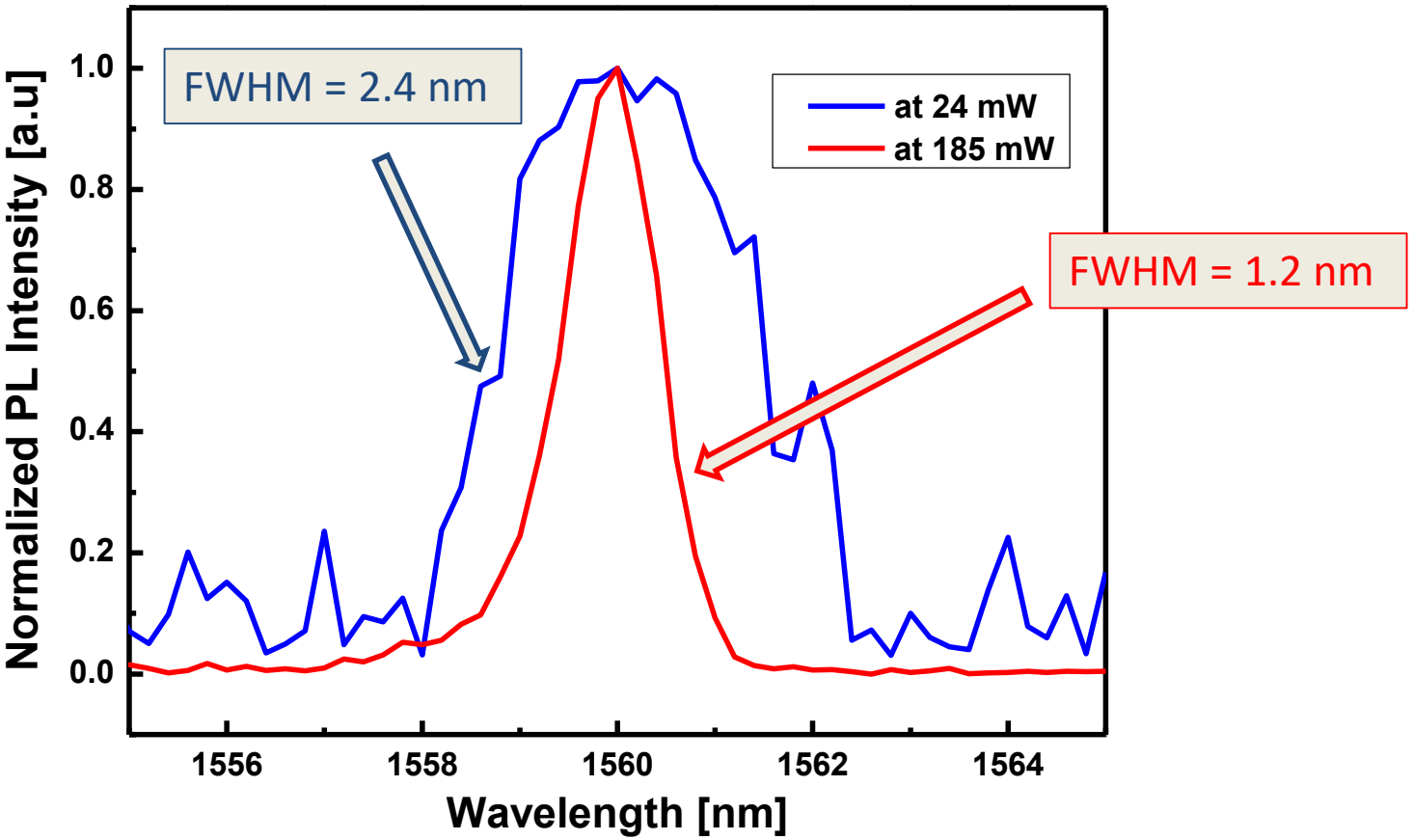

$^4I_{13/2} \rightarrow {}^4I_{15/2}$ photoluminescence spectrum of the cavity activated by Er^{3+} ions in 1D dielectric microcavity. The emission is recorded at 0 degree from the normal on the samples upon excitation at 514.5 nm at the input power of 185 mW (red line) and 24 mW (blue line). 30 degree of excitation angle for both the measurements.

Peak intensity and FWHM vs Pump Power
Exciting at 514.5 nm / 30°

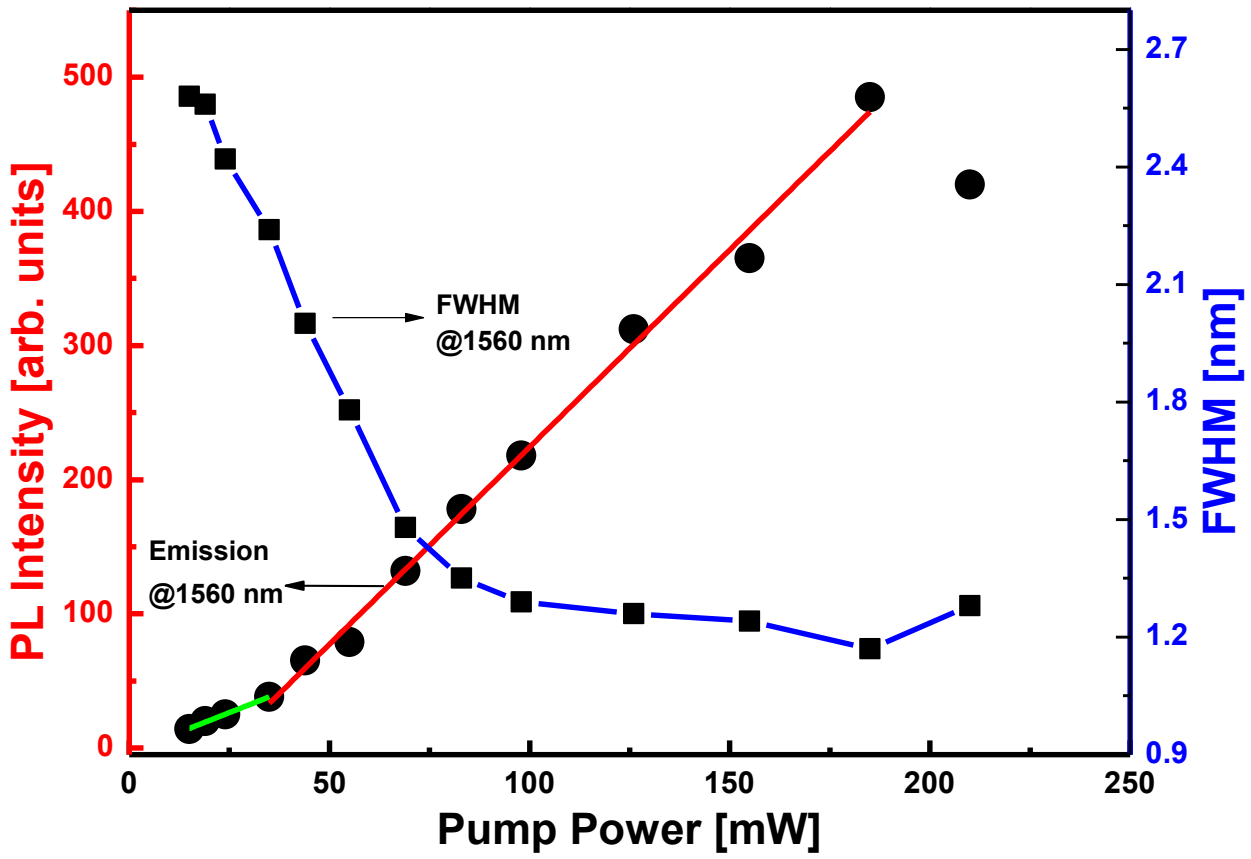

$^4I_{13/2} \rightarrow {}^4I_{15/2}$ photoluminescence peak intensity and FWHM (blue line) at 1560 nm as a function of 514.5 nm pump power with 0 degree of detection angle and 30 degree of excitation angle. Red and green line are the results of linear fit while the blue line is a guide for the eyes.

Peak intensity and FWHM vs Pump Power
Exciting at 514.5 nm / ≠ 30°

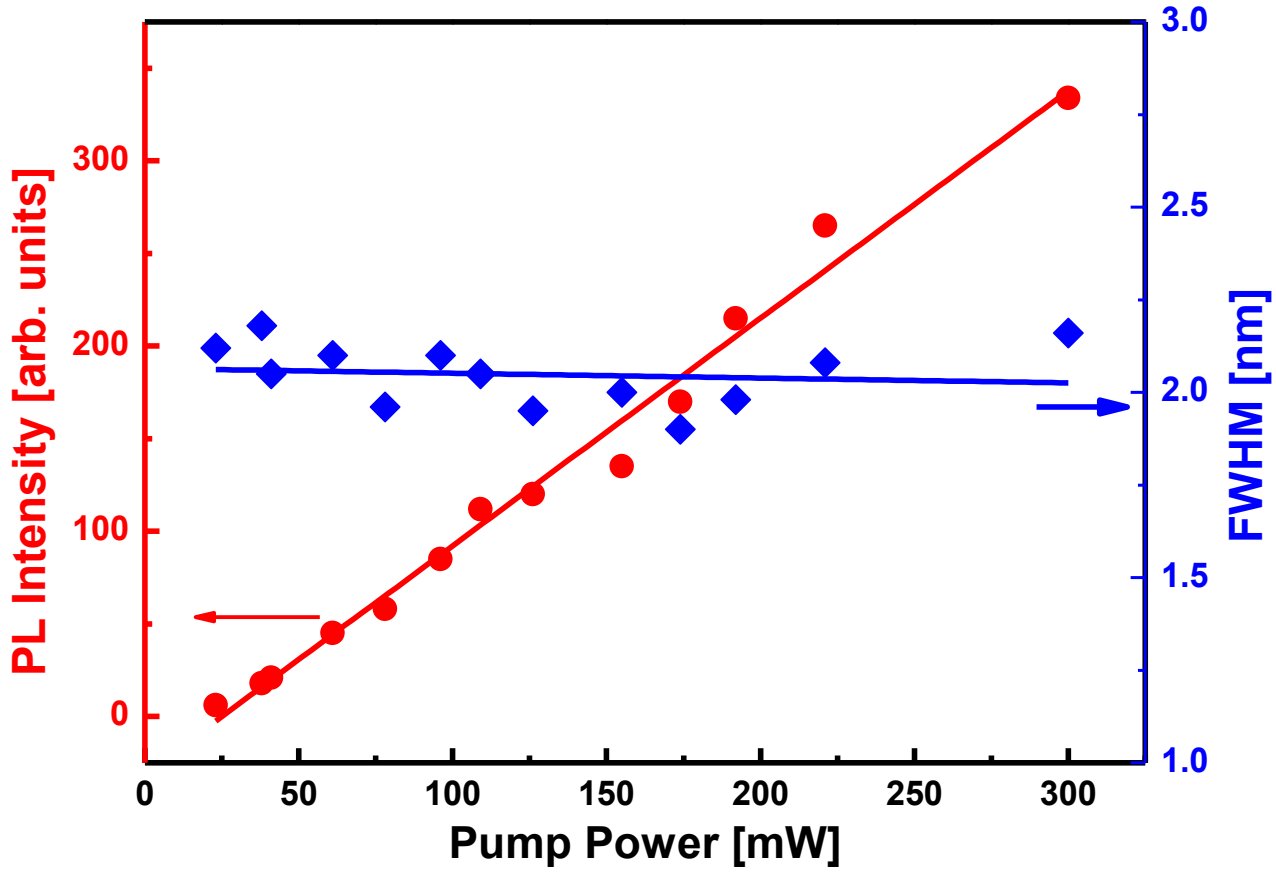

$^4I_{13/2} \rightarrow {}^4I_{15/2}$ photoluminescence peak intensity and FWHM (blue line) at 1560 nm as a function of 514.5 nm pump power with 0 degree of detection angle and 45 degree of excitation angle. Red and blue line are the results of linear fit.

Peak intensity and FWHM vs Pump Power
Exciting at 980 nm / 30°

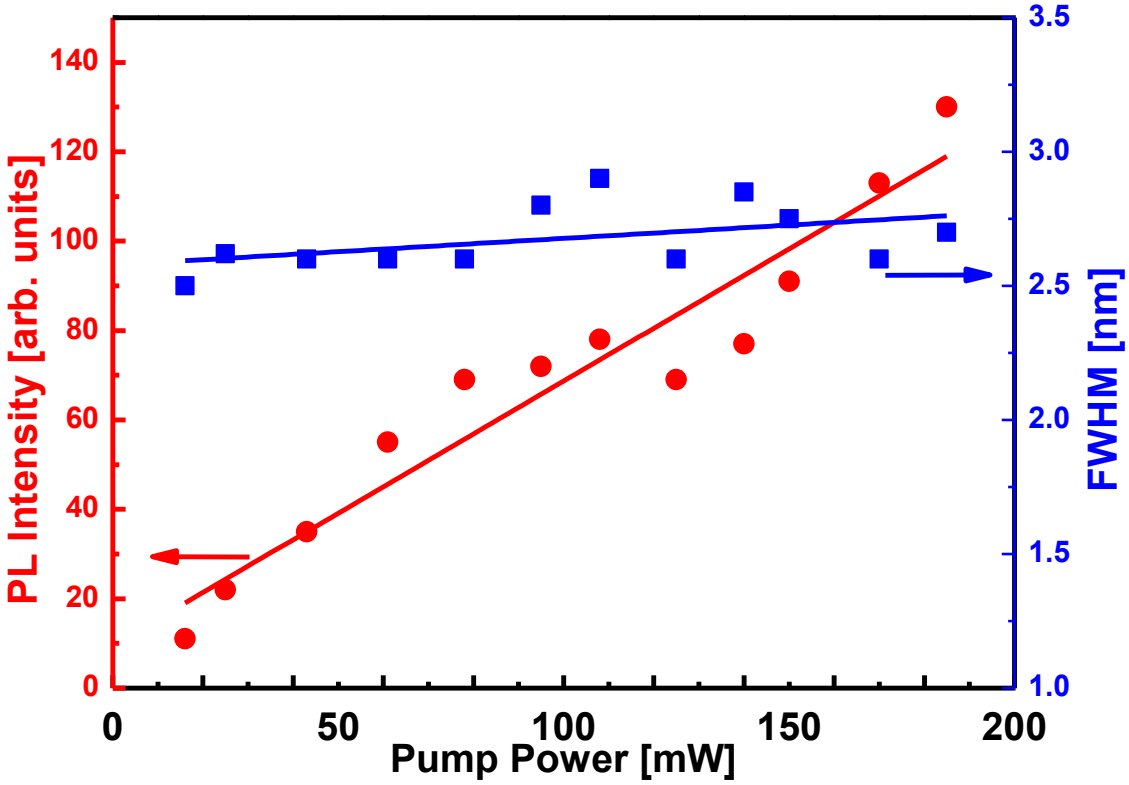

$^4I_{13/2} \rightarrow {}^4I_{15/2}$ photoluminescence peak intensity (red) and FWHM (blue) at 1560 nm as a function of 980 nm pump power with 0 degree of detection angle and 30 degree of excitation angle. The blue and red lines are the results of linear fit.

Conclusions

- Photonic crystals that exhibit specific morphologic, structural, and optical properties allow to develop interesting new physical concepts, as well as novel photonic devices based on the control of the light.

- The cavity is designed to present a cavity resonance at 1560 nm at 0° of detection that correspond to the $^4I_{13/2} \rightarrow {}^4I_{15/2}$ Er^{3+} ions emission and a third order resonance placed at around 514 nm with 30° of incidence from the normal of the sample that is used to pump the sample with an Ar+ laser line.

- The behavior of the emission intensity at emission wavelength of 1560 nm and FWHM as a function of different 514.5 nm excitation powers, with a detection angle of 0° and an excitation angle of 30°, is nonlinear. Simultaneously there is a narrowing of the FWHM from 2.5 nm at low pump power to approximately 1 nm, which is limited by a spectral resolution of our experimental set up with a threshold power of 30 mW.

Acknowledgement

This research is performed in the framework of the projects:
COST MP1401 “Advanced Fibre Laser and Coherent Source as tools for Society, Manufacturing and Lifescience” (2014 – 2018),
ERANET-LAC FP7 Project RECOLA - Recovery of Lanthanides and other Metals from WEEE (2017-2019) ,
MiFo Centro Fermi (2017-2018).